Design and Evaluation of a Pole Placement Controller for Controlling Vibration of Structures

Xia Pan, Stephen Moore and James A. Forrest

Maritime Platforms Division, Defence Science and Technology Organisation
506 Lorimer Street, Fishermans Bend, Victoria 3207, Australia

ABSTRACT

This paper discusses the design and evaluation of a pole placement controller for reducing vibration of structures. The design of the controller involves shifting the poles of a transfer function describing the structure's dynamic behaviour by using a feedback control gain. The feedback control gain is chosen to minimise the vibration response of the structure. The performance of the controller is evaluated by simulation using a dynamic model of a plate estimated from experimental data. The experimental data consisting of natural frequencies, structural damping and eigenvectors are used to construct a state-space model where the state vector is multiplied by the control gain to produce a control input. The effect of pole location and the effect of excitation type on structural response and control signal required are discussed in detail. Also, the effect of measurement noise on the robustness of the controller is investigated. Results show that the controller produces a significant reduction in the plate vibration.

INTRODUCTION

Vibration control of structures is an important issue in many applications. Active control of vibration and sound radiation from flat plates are examples which have received considerable attention in the past and will continue to do so in the future, as flat plates are the basic building blocks of many engineering structures, including the hull of a marine vessel.

Early work on active feedforward control of vibration of plates was investigated by rearranging the vibration field (Pan & Hansen 1995 and Johnson & Elliot 1995). Recently, control systems have increasingly used feedback control to damp the vibration rather than a feedforward arrangement, because of its ability to deal with broadband random vibration without an external reference signal. Gardonio and Elliott (2004) reviewed the decentralized feedback control approach for a smart panel with different types of transducers. Pan and Forrest (2010) extended their work on control of sound radiation from a smart panel to any size of flat plate. The latter work assumed that an appropriate controller is available.

An overview of essential aspects involved in the design of an active vibration control system can be found in Alkhatib and Golnaraghi (2003). One of the key issues is to design the controller. A survey of the issues of digital controller implementation was presented by Hanselmann (1987). Various controllers can be designed such as proportional-plus-integral, linear quadratic regulator, or pole placement. The poles are related to the damped natural frequencies of the system. The pole placement method was chosen for the current study, as it is one of the simple but effective methods for multimodal active vibration suppression (Sethi & Song 2006). The pole placement control system can be realised by applying a simple feedback control gain matrix, and the gain matrix is based on a dynamic model which produces a fast response to the system through control actuators. The pole placement method is also known as a direct time control technique with closed loop poles (Marium *et al*. 2005).

The pole placement control has been successfully implemented by Manning *et al*. (2000), Scott *et al*. (2001) and Bu *et al*. (2003) for controlling the first dominant mode of flexible beams. Sethi and Song (2005) implemented the pole placement for controlling the first three modes of flexible beams by using a single sensor and a single actuator. In their experimental set up, system identification for the dynamics of the first three modes and model reduction techniques were employed to assist the control system design. Sethi and Song (2006) then extended their work on pole placement control of vibration of beams to a smart model frame structure (a three-storey model for simulating civil structures from dynamic loading under severe winds and earthquakes). Their experimental results demonstrated the effectiveness of multimodal vibration control of the smart frame structure using the pole placement method. Kumar and Khan (2007) and Kumar (2010) designed controllers based on the adaptive and robust pole placement method, and implemented the controllers on an inverted L beam. They indicated the adaptive pole placement controllers were noise tolerant, but required high actuator voltages to maintain stability. They also showed the robust pole placement controllers required comparatively small amplitude of control voltages to maintain stability, but were noise sensitive.

The key goals for the current paper are:

(1) design of a pole placement controller for any vibrating structure

(2) evaluation of the performance of the controller for controlling vibration of structures

(3) investigation of the effect of pole location and the

This paper has been approved for public release by the Chief of Maritime Platforms Division, DSTO.

effect of excitation type on structural response and control input required; and

(4) investigation of the effect of signal noise on the performance of the controller.

EXPERIMENTAL ARRANGEMENT AND RESULTS

A flat steel plate with dimensions 1440 × 710 × 3 mm (area 1 m^2) was tested. The plate was freely suspended from a heavy steel frame (Figure 1). Vibration response measurements were obtained using a Polytec PSV-400-3D scanning laser vibrometer. Only out-of-plane (z direction) data have been considered in this study. There were 135 measurement points, as shown in Figure 2. Point 19, marked by the arrow and red dot in the figure, was excited by an electrodynamic shaker. The excitation force was measured using a Brüel & Kjær 8201 force transducer. The modal parameters (natural frequencies, damping, and mode shapes) were extracted using a non-linear least squares algorithm implemented in the ICATS v2003 suite of modal analysis software.

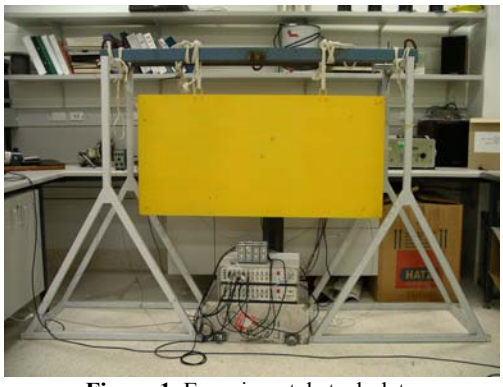

Figure 1. Experimental steel plate.

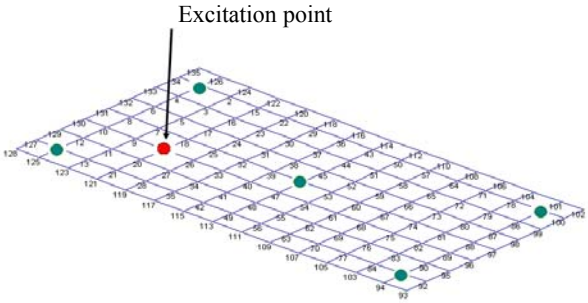

Figure 2. Arrangement of measurement points on the plate. ●, primary excitation; ●, response measurement points for simulation.

Table 1 lists measured natural frequencies and structural damping for the first ten non-rigid body modes. Figure 3 shows the corresponding mode shapes for these first ten modes. The modes are determined for the experimental setup with the plate, suspended by two ropes, which is close to free-free-free-free but not quite. The rigid-body modes are then the plate swinging on the ropes, rather than free motion through space. The fundamental mode (mode 1) and its counterpart mode (mode 7) are characterised by two parallel nodal lines, and other modes are characterised by more complicate nodal lines for the plate. The swinging rigid-body modes together with the modes shown in Figure 3 indicate the behaviour of the free-free-free-free plate in the experiment. These modal parameters were all calculated in the ICATS software based on the measured responses at all 135 points on the plate. For the control system simulation, the responses at only 5 of these points were considered. These points are marked with green dots in Figure 2.

Table 1. Natural frequencies and structural damping

Mode	Natural Frequency (Hz)	Damping (structural damping)
1	15.4	9.1E-03
2	23.2	1.1E-02
3	37.6	1.0E-03
4	44.8	2.0E-04
5	61.2	1.1E-03
6	70.1	2.0E-04
7	72.0	1.1E-03
8	73.2	6.0E-04
9	107.0	5.0E-04
10	118.1	3.0E-04

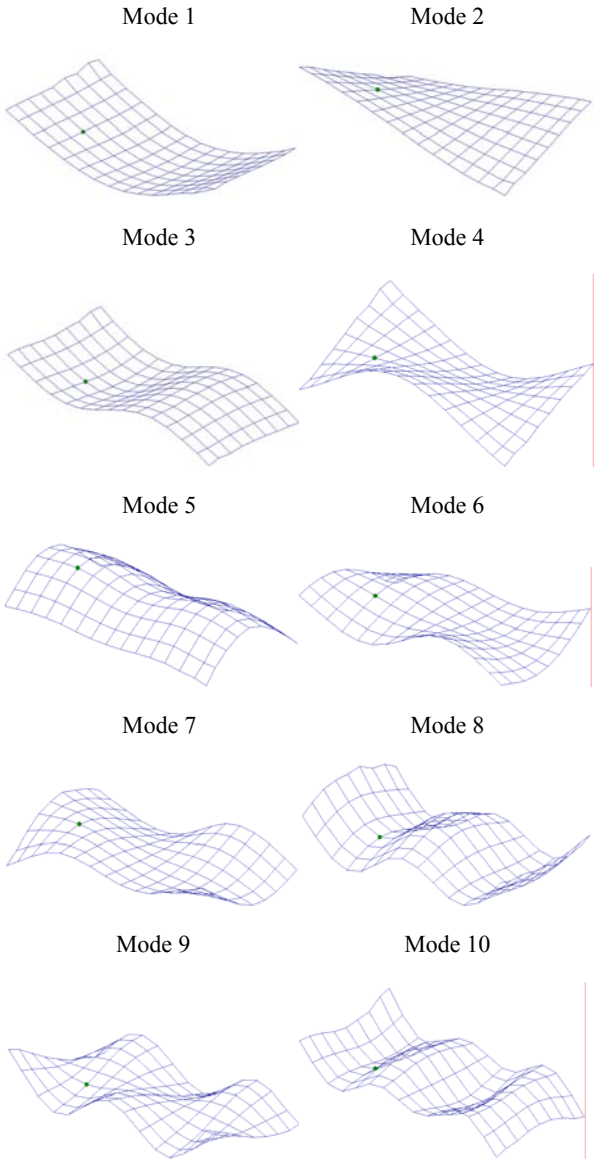

Figure 3. Measured mode shapes of the first ten modes.

STATE-SPACE REPRESENTATION AND POLE PLACEMENT

Consider a state space representation of a multiple degree-of-freedom system of order n

$$\dot{\mathbf{x}} = \mathbf{A}\mathbf{x} + \mathbf{B}\mathbf{u} \quad (1a)$$

and

$$\mathbf{y} = \mathbf{C}\mathbf{x} \quad (1b)$$

where

$\mathbf{x} = n \times 1$ state vector
$\mathbf{u} = l \times 1$ vector of l system inputs or total input
$\mathbf{A} = n \times n$ state matrix
$\mathbf{B} = n \times l$ input matrix
$\mathbf{C} = m \times n$ output matrix of m structural outputs
$\mathbf{y} = m \times 1$ output vector.

A, B and **C** will be named state (parameter) matrices. We can choose the control signal to be

$$\mathbf{u} = -\mathbf{K}\mathbf{x} \quad (2)$$

where **K** is a $(l \times n)$ feedback control gain matrix. Equation (2) shows the control signal is determined by the instantaneous state of the system. Substituting Equation (2) into Equation 1(a) gives

$$\dot{\mathbf{x}}(t) = (\mathbf{A} - \mathbf{B}\mathbf{K})\mathbf{x}(t). \quad (3)$$

The solution of this equation is given by

$$\mathbf{x}(t) = e^{(\mathbf{A}-\mathbf{B}\mathbf{K})t}\mathbf{x}(0) \quad (4)$$

where $\mathbf{x}(0)$ is the initial state. The stability and transient response characteristics are determined by the eigenvalues of matrix $\mathbf{A} - \mathbf{B}\mathbf{K}$ (Ogata 1997). For $\mathbf{x}(0) \neq 0$ and **K** chosen properly, it is theoretically possible to make $\mathbf{x}(t)$ approach 0 as t approaches infinity. The eigenvalues of matrix $\mathbf{A} - \mathbf{B}\mathbf{K}$ determine the new (desired) poles of the system. The gains **K** are chosen to increase the damping associated with each resonance, recalling that the poles are related to the damped natural frequencies of the system.

Figure 4(a) shows a block diagram representation of the state-space Equations (1) and Figure 4(b) shows a block diagram of the same system with a feedback control gain applied. For a single-input system, a procedure for calculating a pole placement controller was given by Ogata (1997) using known desired poles to determine the feedback control gain. This procedure involves the following five steps:

(1) check the controllability condition for the system;

(2) determine the coefficients of the characteristic polynomial for matrix **A**;

(3) determine the transformation matrix **T** that transforms the system state equation into the controllable canonical form (Ogata 1997);

(4) using the desired poles, write the desired characteristic polynomial and determine its coefficients;

(5) the required state feedback gain vector is then determined from the difference of the coefficients obtained in step 4 and the corresponding coefficients obtained in step 2, multiplied by the inverse of the matrix **T**.

If the system is controllable, the above procedure can be replaced by using a Matlab function "place". Note that "place" uses an algorithm (Kautsky 1985) for multi-input systems and is recommended for single-input systems as well.

(a)

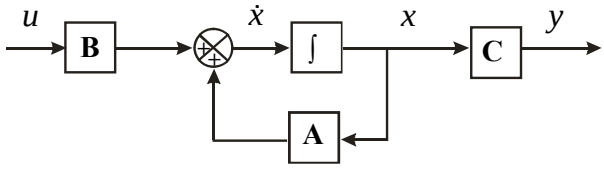

(b)

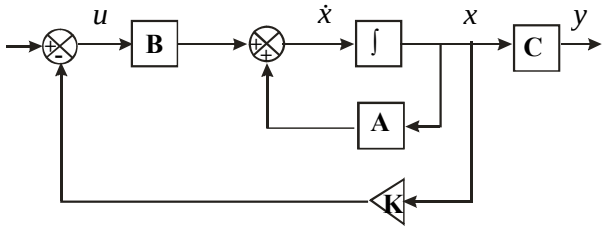

Figure 4. Block diagrams for (a) the state-space representation; and (b) the control system using feedback gain.

DETERMINATION OF FEEDBACK CONTROL GAIN FOR THE CURRENT SYSTEM

The dynamic behaviour of the plate was modelled using a state-space description with the parameter matrices calculated from the experimentally determined modal parameters. The state-space model was implemented in Simulink. This procedure involved the following four steps:

(1) calculate poles and residues of a transfer function describing the dynamic properties of the plate (i.e. pole-residue representation of the uncontrolled system), based on the experimental natural frequencies and modal damping, and the mode shapes;

(2) determine a state-space model of the uncontrolled system based on the uncontrolled poles and residues. Assess the controllability of the system;

(3) calculate desired poles from the uncontrolled poles and desired damping ratio; and

(4) calculate the state feedback control gain using desired poles, and state matrices from the uncontrolled system.

Some specific steps will be described in the following. In the following discussions, a single-input system is assumed for the reason of simplicity. The equations below follow the approach described by Maia & Silva (1997). The transfer function at point *i* on the plate in pole residue form can be written as

$$h_i(s) = \sum_{j=1}^{n} \frac{r_{ij}}{s - p_j} + \frac{r_{ij}^*}{s - p_j^*} \qquad (5)$$

where r_{ij} is the element of a $(m \times n)$ residue matrix and p_j is the element of a $(n \times 1)$ column vector of pole locations, *s* is the Laplace transform variable (related to frequency), and star denotes the complex conjugate.

For an underdamped system, the poles at mode *j* can be written as

$$p_j = -\zeta\omega_j + i\omega_j\sqrt{1-\zeta^2} \qquad (6)$$

where ω_j is the natural frequency and ζ is the damping ratio. The expression relating damping ratio and structural damping β is

$$\zeta = \frac{\beta}{2}. \qquad (7)$$

Assuming eigenvectors Φ are mass normalized, the residue at point *i* with a primary excitation at point *0* is

$$r_{ij} = \Phi_{0j}\Phi_{ij}. \qquad (8)$$

The transfer function is then obtained by substituting r_{ij} together with the existing poles p_j obtained from Equation (6) into Equation (5). The transfer function is then used to determine the state-space model. Transformation from a transfer function form to a state-space representation is easily done using functions provided in Matlab.

A pole placement controller can only be implemented for a controllable system. The system controllability can be tested by determining the rank of a controllability matrix $[\mathbf{B} \mid \mathbf{AB} \mid ... \mid \mathbf{A}^{n-1}\mathbf{B}]$. If the rank of the controllability matrix is *n*, the system is stable and pole placement techniques can be applied to the system (Ogata 1997).

Desired poles are determined by using the existing natural frequency and changing the damping. This can be obtained by substituting the natural frequency and desired damping ratio into Equation (6).

For plate responses measured at *m* points, the poles at each of the *m* points are the same. However, the residues are different at each point (see Equation (8)). The responses at the *m* points are calculated individually by determining *m* transfer functions (see Equation (5)). Thus, the total transfer function is a combination of the *m* transfer functions, which can be used to determine the resulting state-space model and the feedback control gain.

COMPLETE SYSTEM DESIGN VIA POLE PLACEMENT CONTORL

Figure 5 shows a block diagram of the Simulink model used in this study. The primary excitation to the system is either a unit step function or a sine function at 15.4 Hz (the natural frequency at the first mode). The top part of the figure consists of the primary input directly exciting the structure to produce an uncontrolled output response. The lower part of the block diagram represents the controlled structure. The control system consists of a feedback loop implementing the control gain. The control gain is multiplied by the state vector to produce a control input. The total input *u* to the structure is then the difference of the primary input and the control input, which minimizes the structure's response. The block diagram also includes display blocks to capture the input and output data from both the uncontrolled and controlled systems. The input and output data are compared for a number of cases discussed in the following section.

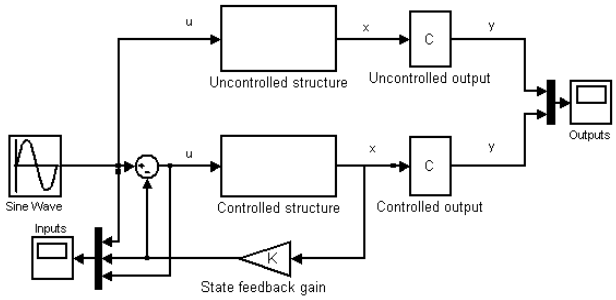

Figure 5. Simulink model showing the complete system design via pole placement. Both uncontrolled and controlled systems are shown in the one diagram. The scope blocks labelled "Inputs" and "Outputs" are simply for monitoring all the input and output signals respectively.

SIMULATION RESULTS

The following simulation is an extension of the work done by Pan and Forrest (2010) on a simply supported plate with the same dimensions and properties as the current plate. They showed that using either a control actuator located at the centre of the plate or four control actuators located near four corners of the plate could reduce vibration and sound radiation from the plate through an active control approach. Therefore, the plate responses at those locations will be determined for evaluating the performance of the controller in this paper. Referring to Figure 2, the results of plate responses at the centre (point 46) and four corners (points 1, 14, 85 and 91) of the plate will be presented separately for comparing with future experimental results. The first ten non-rigid body modes were included in the calculation of the state-space model and the poles at the first ten modes of the uncontrolled system were used to calculate the state feedback gain matrix.

In all controlled cases shown below, the desired damping ratio was 0.7 for calculating desired poles at all modes. This is because for a second order system this damping ratio

provides an overshoot less than 5%. Also, the maximum overshoot and the rise time conflict with each other (Ogata 1997). In other words, both the maximum overshoot and the rise time cannot be made smaller simultaneously. This damping ratio and the resulting rise time are a compromise with each other (see the example given by Ogata (1997)). A multiple degree-of-freedom system can be thought of as a sum of second order systems that are defined over a limited frequency range, i.e. a sum of modes. Therefore, this damping ratio applied to all modes will be assumed to yield a desirable response for the multiple degree-of-freedom system.

Central plate response

In this section, the simulation results were obtained at the centre of the plate. Figures 6(a) and (b) show the pole-zero maps before and after control respectively. Before control, all the poles are located close to the imaginary axis, corresponding to the lightly-damped modes of the uncontrolled structure. After control, all the poles are moved to the left-half s-plane as a result of increasing the damping. The two different sets of pole locations shown in Figures 6(a) and 6(b) will result in different structural outputs which will be described below. Note that the zero locations are not changed after control. Also, the pole locations shown in the pole-zero maps are the same for any measuring point as mentioned previously. The gain matrix **K** is a vector in this case and the values of gain in it range from 1.27×10^3 to 1.26×10^5 for this solution.

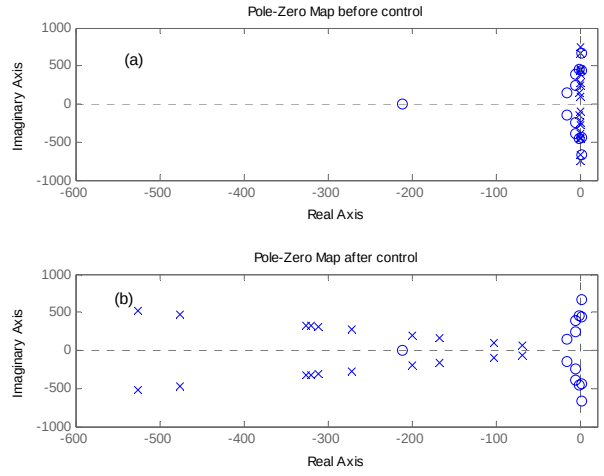

Figure 6. Pole-zero maps before and after control (a) before control; (b) after control. ×, poles; ○, zeros.

Figure 7 shows the transfer functions relating the response at the plate centre to the excitation before and after control. The input is force and the output is acceleration. Thus, the reference level of the dB magnitude scale is 1 ms^{-2}/N. By moving the poles to the left-half s-plane, the magnitude of the transfer function is reduced more than 30 dB at all the resonances except for the first resonance where a reduction of 18 dB is obtained. This is because the uncontrolled damping ratio at the first resonance is larger than those at the other resonances. Thus, applying the same controlled damping ratio to all resonances we would expect less damping effect on the first resonance. The results in Figure 7 were generated by changing the sine input signal block shown in Figure 5 to a band-limited random input with a bandwidth of 200 Hz. The model was run for 20 seconds and input and output time series stored. The transfer functions were calculated as the ratio of the power spectral density (PSD) of the output divided by the PSD of the input, using 8 averages in each case.

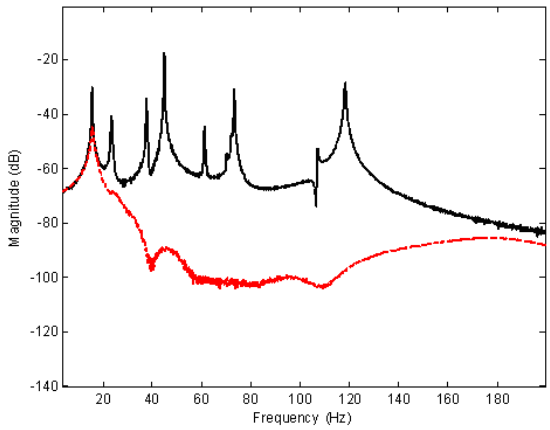

Figure 7. Transfer function at the plate centre before and after control. ─, before control; - - -, after control.

The transient results were obtained by running the model in Figure 5 with the state matrices and control gain calculated previously. Figures 8(a) and (b) show the controlled and uncontrolled structural inputs and outputs due to the step excitation. Before control, all the poles (see Figure 6(a)) generate an oscillatory output with amplitude determined by the initial conditions (see black solid line in Figure 8(b)). The response of the controlled system is heavily damped and settles to a non-zero steady state value (see red dashed line in Figure 8(b)).

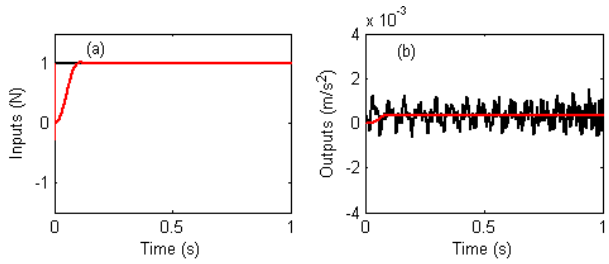

Figure 8. Inputs and outputs at the plate centre due to step excitation (a) inputs; (b) outputs; ─, before control; - - -, after control.

Figure 9 shows the controlled and uncontrolled structural inputs and outputs due to sine excitation at a frequency equal to that of the first mode. Two time ranges 0-10 seconds (Figures 9(a) and 9(b)) and 0-1 second (Figures 9(c) and 9(d)) are presented. Figure 9(a) shows the controlled input signal relative to the primary input signal. Figure 9(b) shows that the uncontrolled system takes about six seconds to reach a steady state level. Note that if the sine excitation is off the resonance the uncontrolled system reaches the steady state

level much quicker. A significant reduction of the output is achieved by the controller and the settling time is reduced rapidly. More detailed transient results can be observed in Figures 9(c) and 9(d).

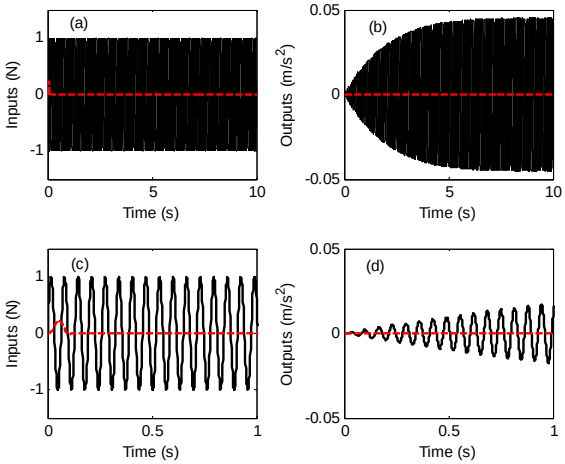

Figure 9. Inputs and outputs at the plate centre due to sine excitation at the first mode (a) inputs plotted 0-10 seconds; (b) outputs plotted 0-10 seconds; (c) inputs plotted 0-1 second; (d) outputs plotted 0-1 second. ─, before control; - - -, after control.

Corner plate response

In this section, the controlled and uncontrolled structural outputs at four corners of the plate due to different types of primary excitations will be presented. The pole locations are the same as those shown in Figure 6. The structural inputs are the same as those shown in Figure 8(a) and Figure 9(c) for the step and sine excitations respectively. These results will not be repeated here. Due to the state-space model now including the four corner responses, the gains differ from the single output case. The values of gain in the gain matrix **K** now range from 6.36×10^2 to 6.32×10^4 to achieve the controlled poles shown in Figure 6(b).

Figure 10 presents the outputs due to the step excitation. The feedback control gain, implementing the desired pole locations, effectively increases damping to the system and reduces the settling time at each corner. With control (red dashed line), different steady state values of each corner can be observed which are due to the residues of the controlled system and because the step excitation has a non-zero mean (DC) component. The steady state response in each corner due to sine excitation is reduced as shown in Figure 11 below. Results shown in Figure 11 follow a similar trend to those at the plate centre as shown in Figure 9(d)

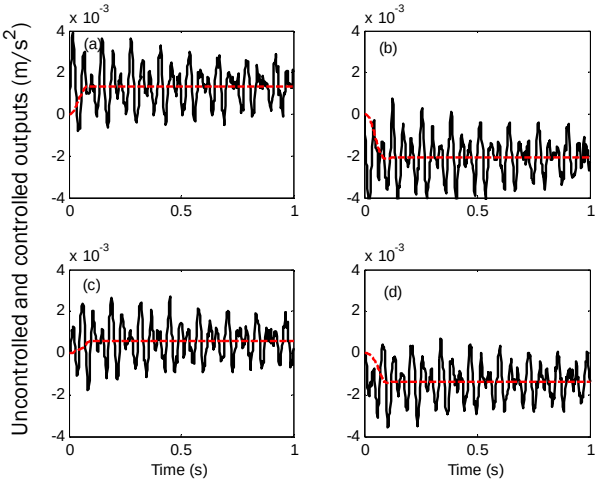

Figure 10. Structural outputs at the plate corners due to step excitation (a) outputs at point 1; (b) outputs at point 14; (c) outputs at point 85; (d) outputs at point 91. ─, before control; - - -, after control.

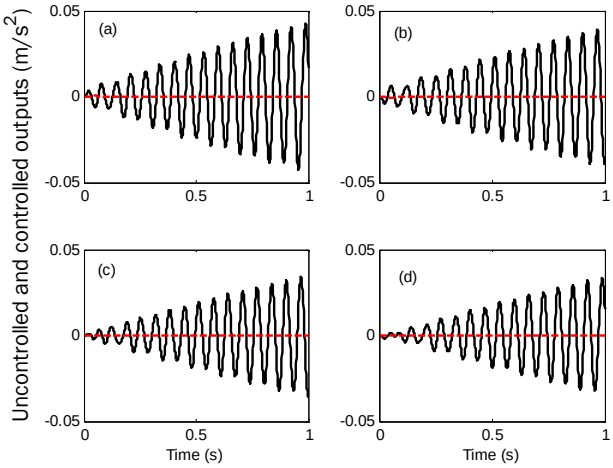

Figure 11. Structural outputs at the plate corners due to sine excitation at the first mode (a) outputs at point 1; (b) outputs at point 14; (c) outputs at point 85; (d) outputs at point 91. ─, before control; - - -, after control.

The performance of the controller was also tested using a random excitation signal. As expected, the controller significantly damped the structural response but a larger feedback control signal was required. While the control signal for a sine excitation had a similar peak-to-peak level as the external excitation, the control signal for random excitation was about 1.5 times the excitation peak-to-peak level. Thus, the pole placement technique can be applied to structures excited by any primary source as the control law is the same for any primary excitation. However, the control signal required is dependent upon the excitation type. Note that the control actuator should not be located on the nodal lines of the modes to be controlled (Pan & Forrest 2010), as the location of the control actuator affects the control gain. An infinite control gain would be required if the control actuator is located on the nodal lines. In practice, one can move the control actuator experimentally to avoid being located on the nodal lines.

Effect of measurement noise on the performance of the controller

In practice, it is common that measurement noise affects the signals in the error vector (error sensors) which reduces the performance of the controller. This situation was simulated by adding zero-mean random noise to the state vector (variables). A Simulink model including the measurement noise is shown in Figure 12. Figure 13 shows the results obtained by running Figure 12. The uncontrolled results were obtained previously. Figure 13(a) shows the controlled and uncontrolled outputs at the plate centre due to sine excitation with injected random noise having a standard deviation $\sigma = 4\times10^{-5}\times RMS$ of the state vector. This is the threshold where the "controlled" output is still just less than the uncontrolled output. Figure 13(b) shows the result above the threshold, with the injected random noise set with $\sigma = 6\times10^{-5}\times RMS$ of the state vector. The results indicate the control system becomes unstable and the structural response increases when the measurement noise is above this threshold. This is because the components of the random signal that are negative with respect to the state vector at the output side of the structure give rise to positive feedback when multiplied by the gain in the control system. Various constraints in the physical system, control system and hardware can give rise to perturbations like this random noise. These constraints prevent large feedback gains being properly implemented, e.g. actuators may move out of their linear operating range and ultimately not be able to supply enough force in any case.

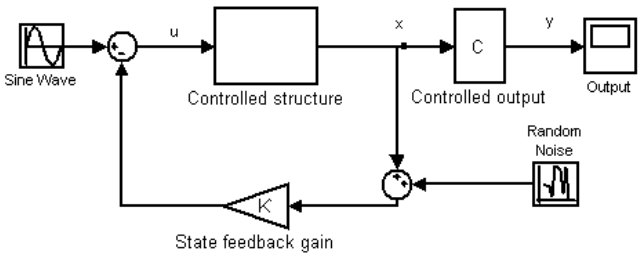

Figure 12. Simulink model including measurement noise added to the state variables.

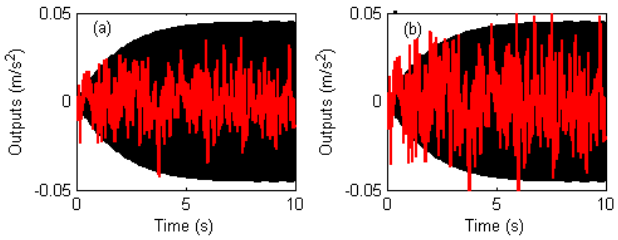

Figure 13. Structural outputs at the plate centre due to sine excitation at the first mode when random noise is present in the state variables (a) at the threshold of system stability; (b) with random noise above the threshold. ─, before control; - - -, after control.

ISSUES AND FUTURE WORK

The major issues in implementing the control system via a pole placement controller are:

(1) The feedback control gain matrix **K** is calculated from the state matrix of the uncontrolled system; in this case modelled using experimental data (natural frequencies, damping and eigenvectors). An accurate model of the structure is required for implementing a pole placement controller.

(2) **K** is not unique for a given system but depends on the desired closed-loop pole locations selected. The selection of the desired pole locations has to be a compromise between the speed of the response of the error vector and the sensitivity to disturbance and measurement noises (Ogata 1997).

(3) In a high-order problem, some choices of pole locations result in very large gains. The further a control system has to push a pole from its original position, the greater the required control input or 'effort'. If the control effort is too large, the control actuator will saturate. The actual system response may look nothing like the desired system response, and may even be unstable when this happens (Hansen & Snyder 1997).

(4) The present pole placement approach specifies the first ten closed-loop poles. There is a cost associated with placing these closed-loop poles (Ogata 1997), because placing them requires successful measurements of all state variables (all elements in the state vector **x**) or else requires the inclusion of a state observer in the system to estimate the state variables.

Therefore, there are several areas for future research. For overcoming all of the first three problems simultaneously, optimal control may be considered (Hansen & Snyder 1997). Rather than beginning with a set of desired pole locations, optimal control takes into account the control effort required to achieve the desired result with the control system.

Decentralised adaptive pole placement control (El-Kashlan & Yousef 1993) could be used to overcome some of the issues with the third problem. In this scheme, multiple semi-independent controllers are used, each controlling one or two poles. This allows the use of lower gains in each controller. Another approach overcoming the third problem is to place the closed-loop poles at certain fixed positions (Kumar 2010). With this approach, the resulting structural response is near a particular value and only a limited control effort is required to maintain system stability.

For overcoming the fourth problem, an approach to pole placement with output feedback instead of the state feedback is proposed. Rather than measuring all state variables, output feedback control only needs to measure outputs as the error vector which can be obtained by using accelerometers, for example. Thus, the output feedback approach would be expected to be a feasible way for implementing pole placement control in a real system.

CONCLUSIONS

The design of a pole placement controller to control vibration of a steel plate has been discussed. As the procedure is

general, it could be applied to design a controller for any vibrating structure once natural frequencies, damping and mode shapes are known. The performance of the controller is evaluated by simulation using a dynamic model of a plate estimated from experimental data. The controller reduces the vibration response of the structure by increasing damping of the system poles. The control technique can be applied to structures excited by any primary excitation; however, the control signal required to damp the structural vibration is dependent upon the excitation type and sensitive to noise added to the state vector.

The authors would like to thank Mr Vinh Trinh for his support in providing the experimental data, and Dr Alex Cave for useful discussions.

REFERENCES

Alkhatib, R. and Golnaraghi, M.F. 2003, Active Structural Vibration Control: A Review. *Shock Vib. Digest.* **35**(5), 367-383.

Bu, X., Ye, L. and Wang, C. 2003, Active Control of a Flexible Smart Beam Using a System Identification Technique Based on ARMAX. *Smart Mater. Struct*. **12**, 845-850.

El-Kashlan, A. and Yousef, H.A. 1993, Decentralized Adaptive Pole-Placement of Large-Scale Systems. *Proc. IEEE Conference*, Le Touquet, France, 17-20 October, 600-604.

Gardonio, P. and Elliott, S.J. 2004, Smart Panels for Active Structural Acoustic Control. *Smart Mater. Struct*. **13**, 1314-1336.

Hanselmann, H. 1987, Implementation of Digital Controllers–A Survey. *Automatica.* **23**(1), 7-32.

Hansen, C.H. and Snyder, S.D. 1997, *Active Control of Noise and Vibration*. E & FN Spon, London, United Kingdom, 260-368.

Kautsky, J., Nichols, N.K. and Van Dooren, P. 1985, Robust Pole Assignment in Linear State Feedback. *Int. J. Control*. **41**(5), 1129-1155.

Kumar, R. and Khan, M. 2007, Pole Placement Techniques for Active Vibration Control of Smart Structures: A Feasibility Study. *J. Vib. Acoustics* **129**, 601-615.

Kumar, R. 2010, Experimental Implementation of Pole Placement Techniques for Active Vibration Control of Smart Structures. *Proc. IMECS*, Hong Kong, 17-19 March.

Johnson, M.E. and Elliott, S.J. 1995, Active Control of Sound Radiation using Volume Velocity Cancellation. *J. Acoust. Soc. Am.* **98**(4), 2174-2186.

Maia, N.M.M. and Silva, J.M.M. 1997, *Theoretical and Experimental Modal Analysis*. Research Studies Press LTD, Hertfordshire, United Kingdom, 1-32.

Manning, W.J., Plummer, A.R. and Levesley, M.C. 2000, Vibration Control of a Flexible Beam with Integrated Actuators and Sensors. *Smart Mater. Struct*. **9**(6), 932-939.

Marium, N., Hizarm, H. and Izzri, A.W.N. 2005, Design of the Pole Placement Controller for D-STATCOM in Mitigating Three Phase Fault, *Proc. Inaugural IEEE PES Conference*, Durban, South Africa, 11-15 July, 349-355.

Ogata, K. 1997, *Modern Control Engineering*. Third Edition, Prentice-Hall, Inc., London, United Kingdom, 134-895.

Pan, X. and Hansen, C.H. 1995, Active Control of Vibratory Power Radiation along a Semi-Infinite Plate. *J. Sound Vib.* **184**, 585-610.

Pan, X. and Forrest, J.A. 2010, Active Structural Acoustic Control of Sound Radiation from Flat Plates. *Proc. Inter. Cong. Acoust*., Sydney, Australia, 1-4 November.

Scott, R.G., Brown, MD. and Levesley, M. 2001, Pole Placement Control of a Smart Vibrating Beam. *Proc. 8th Int. Cong. Sound and Vib.*, Hong Kong, 387-391.

Sethi, V. and Song, G. 2005, Multimodal Vibration Control of a Flexible Structure Using Piezoceramics. *Proc. Inter. Conf. Advanced Intelligent Mechatronics*, Monterey, California, USA, 24-28 July.

Sethi, V. and Song, G. 2006, Multimode Vibration Control of a Smart Model Frame Structure. *Smart Mater. Struct*. **15**, 473-479.